Bifunctional PDDA-stabilized β-Fe_2O_3 nanocluster for improved photoelectrocatalytic and magnetic field enhancing photocatalytic applications

Maoqi Li [a,b], Jian Wu [b] and Guoliang Shen [a]**

a. School of Petrochemical Engineering, Shenyang University of Technology, Liaoyang 111003, P. R. China

b. Key Laboratory of Magnetic Materials and Devices, Ningbo Institute of Materials Technology and Engineering, Chinese Academy of Sciences, Ningbo, 315201, P. R. China

*Corresponding author's email: jwu@nimte.ac.cn, shengl_shxy@sut.edu.cn

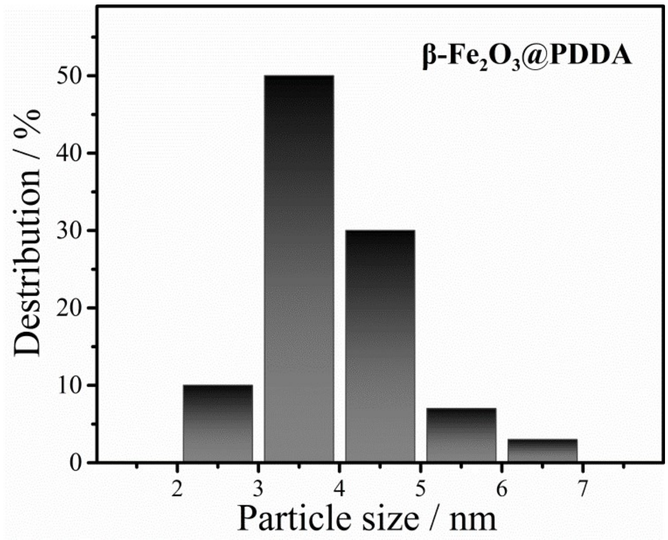

Figure S1. Particle size distribution of β-Fe_2O_3@PDDA.

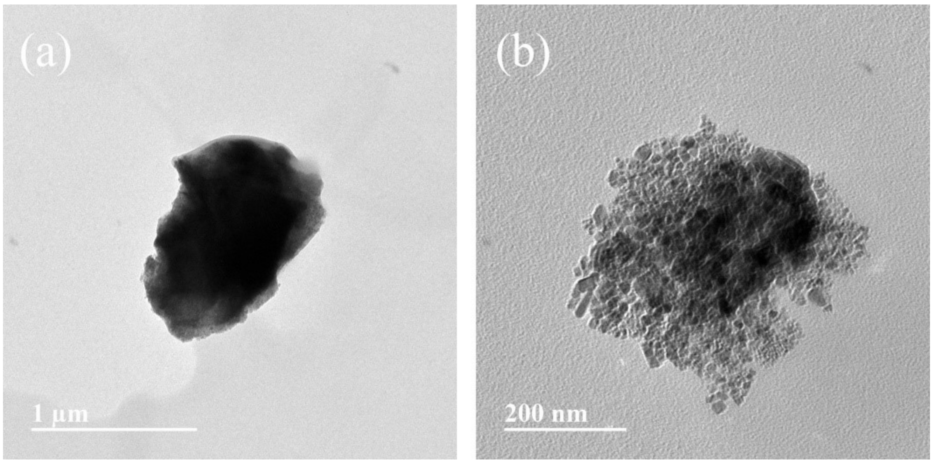

Figure S2. TEM image of bulk α-Fe_2O_3 (a); TEM image of α-Fe_2O_3 nanoparticle (b).

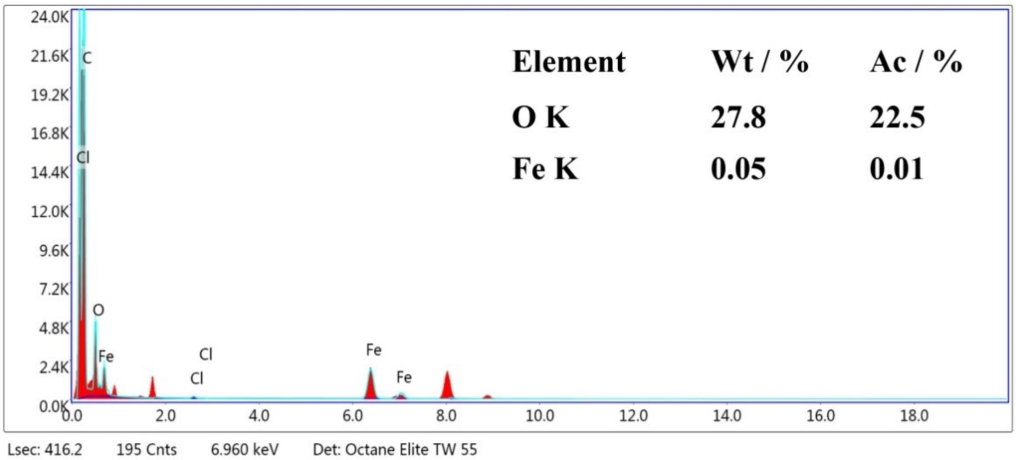

Figure S3. EDS spectrum of β-Fe_2O_3@PDDA.

Table S1. The crystal plane spacing of β-Fe_2O_3@PDDA sample and PDF standard value.

Planes–crystal structure	d-Spacing (Å) PDF#76-1821	crystal plane spacing of β-Fe_2O_3@PDDA sample (nm)	Ratio(%)
(0 0 4)	5.6375	0.56	3
(1 0 0)	4.8151	0.48~0.49	13.8
(1 0 6)	2.9627	0.29~0.32	20.7
(1 1 -1)	2.7591	0.27~0.28	24.1
(1 1 3)	2.6074	0.26~0.27	37.9

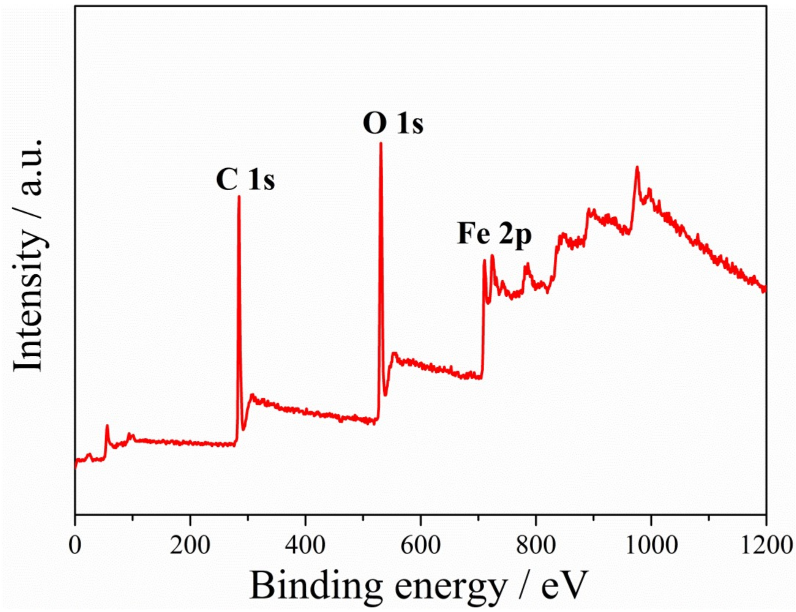

Figure S4. XPS spectra of β-Fe_2O_3@PDDA nanocluster.

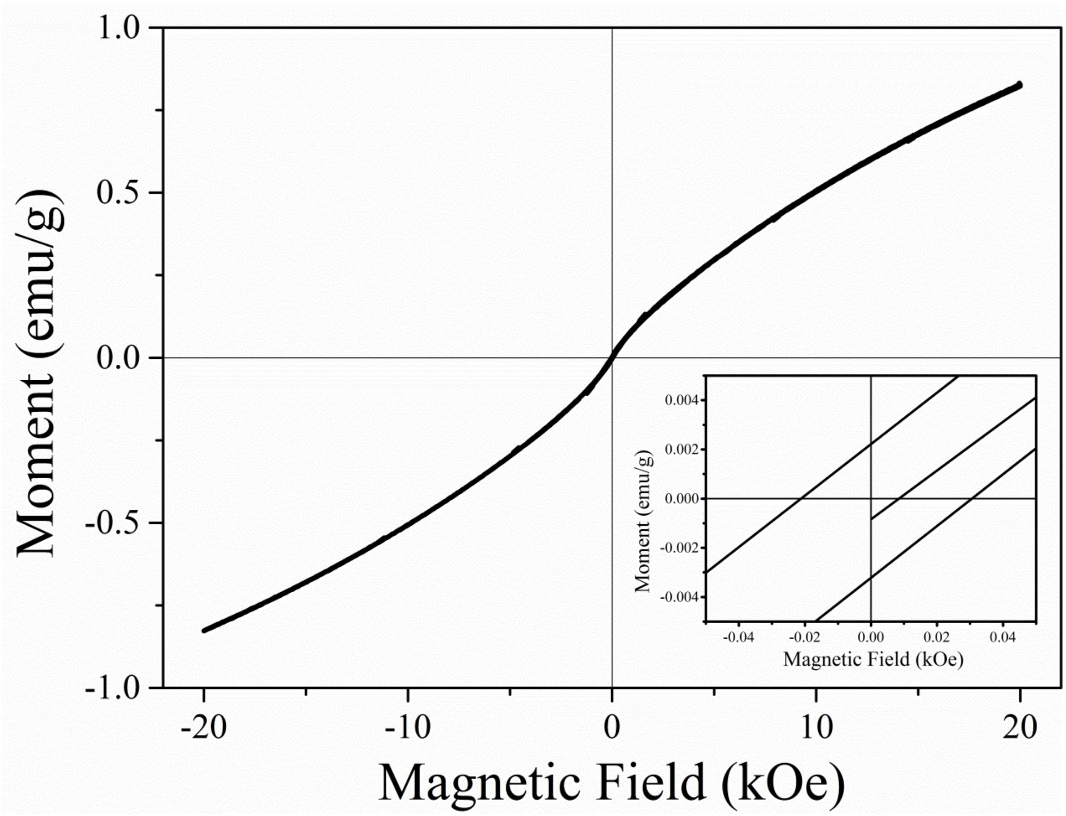

Figure S5. Magnetic hysteresis curve of β-Fe_2O_3@PDDA nanocluster.

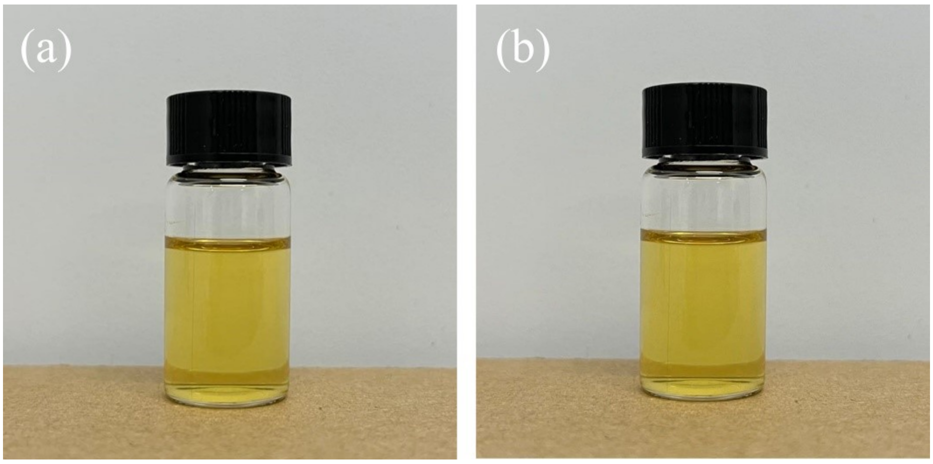

Figure S6. β-Fe_2O_3@PDDA nanocluster samples are uniformly dispersed in aqueous solution(a), and let the solution sit for 10 d(b).

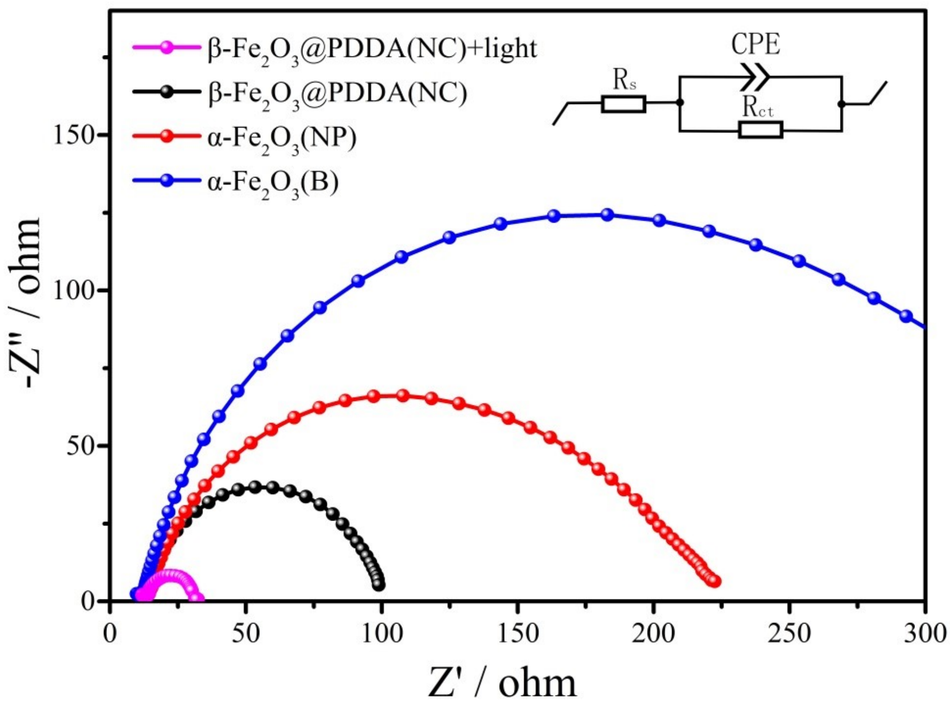

Figure S7. Electrocatalytic impedance spectra (EIS) Nyquist plots(inset:Equivalent circuits of Nyquist plots of materials consisting of three elements: R_s, R_{ct}, and CPE.)

S1. Mass activity and specific activity Calculation.

Mass activities (mA mg^{-1}) of catalysts are calculated based on the catalyst loading (0.25 mg cm^{-2}) and the achieved current density j (mA cm^{-2}) at an η of 520 mV. The corresponding equation is

$$Mass\ activity\ (mA\ mg^{-1}) = \frac{Achieved\ current\ density\ (mA\ cm^{-2})}{Catalyst\ loading\ (mg\ cm^{-2})}$$

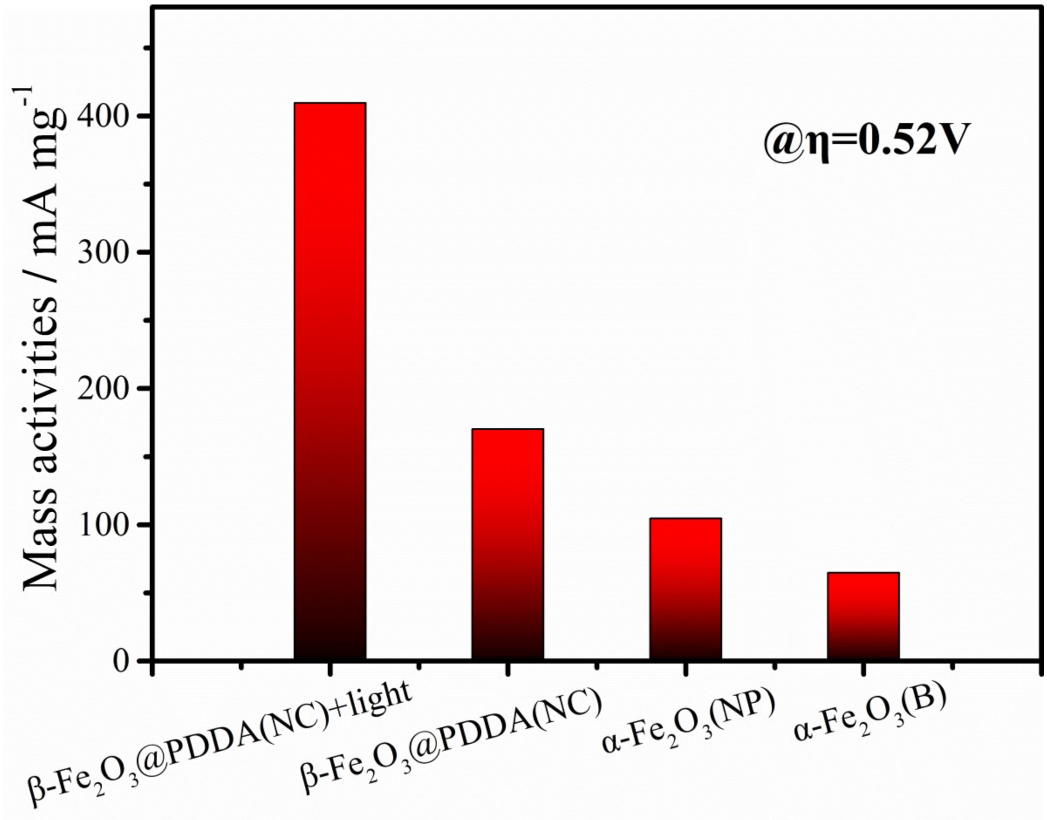

Figure S8. Mass activity (MA) of bulk α-Fe_2O_3, α-Fe_2O_3 nanoparticle, β-Fe_2O_3@PDDA nanocluster and β-Fe_2O_3@PDDA nanocluster under an additional light for OER at an η of 520 mV.

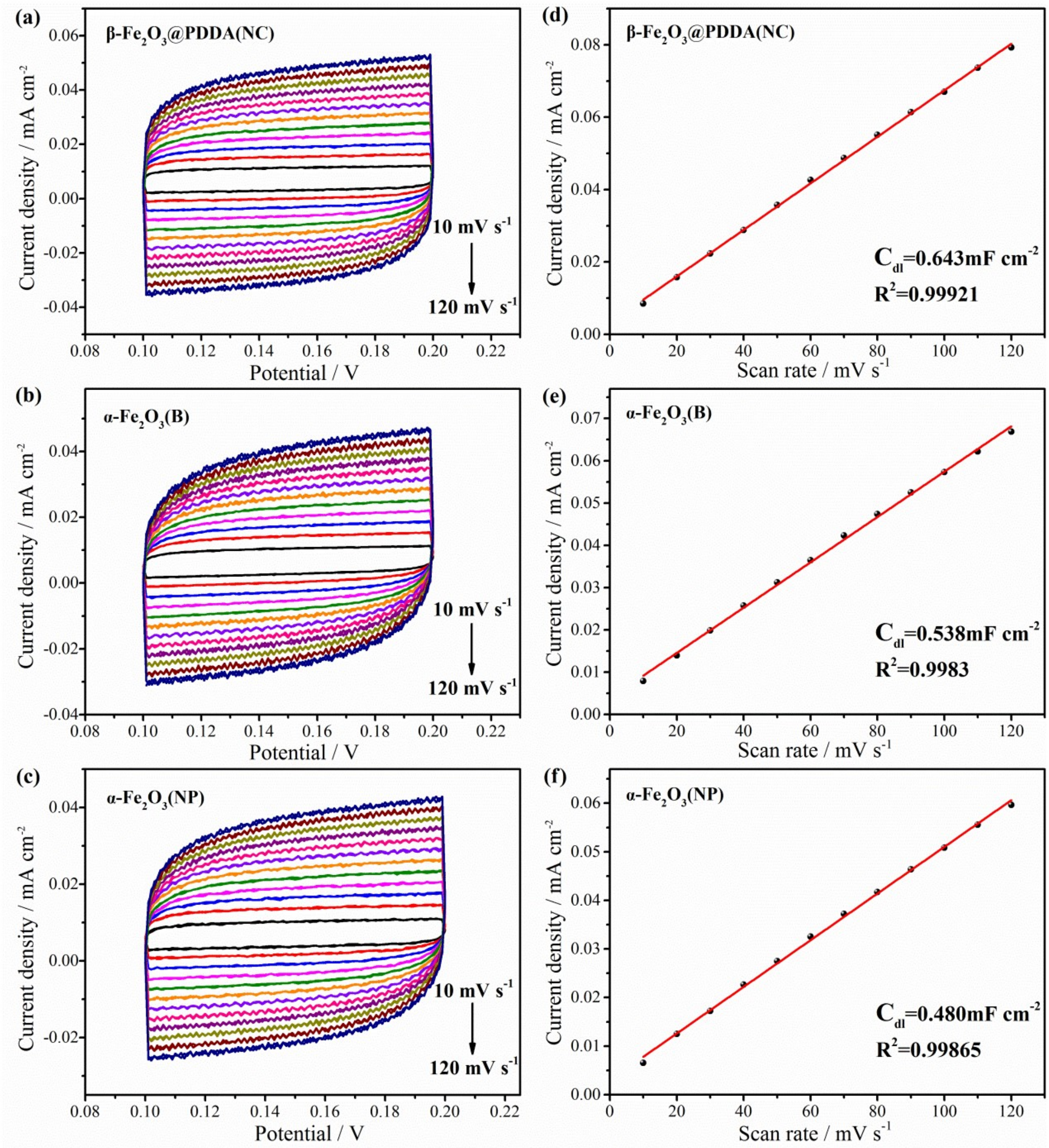

Figure S9. CV curves for (a) β-Fe_2O_3@PDDA nanocluster; (b) bulk α-Fe2O_3; (c) α-Fe_2O_3 nanoparticle in the region of 0.10~0.20 V *vs.* Ag/AgCl with various scan rates (10~120 mV s^{-1}) for OER; Fitting curves for of scanning rate and current density for (d) β-Fe_2O_3@PDDA nanocluster; (e) bulk α-Fe_2O_3; (f) α-Fe2O3 nanoparticle.

Table S2. Comparison of the OER activity for several recently reported active transition metal-based electrocatalysts.

Electrocatalysts	Overpotetial (mV) j=10 mA cm^{-2}	Tafel slope (mV dec^{-1})	Electrolyte (pH)	Reference.
β-Fe_2O_3@PDDA NC (PEC-OER)	300	45	1.0 M KOH	This work
β-Fe_2O_3@PDDA NC	370	77	1.0 M KOH	This work
α-Fe_2O_3 NP	430	107	1.0 M KOH	This work
α-Fe_2O_3 B	460	129	1.0 M KOH	This work
α-Fe_2O_3@g-C_3N_4	425	280	0.5 M KOH	1
γ-Fe_2O_3 NWs	650	~	1.0 M KOH	2
α-Fe_2O_3	310	272	0.1 M KOH	3
Fe_2O_3	440	134	1.0 M KOH	4
Ni-Fe_2O_3	277	68	1.0 M KOH	4
γ-FeOOH	550	~	1.0 M KOH	5
$FeTiO_3$ hollow spheres	420	~	1.0 M KOH	6
NiO	~	242	1.0 M KOH	7
NiOOH	360	111	1.0 M KOH	8
Co_3O_4 Mesoporous	636	~	0.1 M KOH	9
Co_3O_4 Mesoporous	476	~	1.0 M KOH	9
Co_2CrO_4	400	87	1.0 M KOH	10
Co_2CrO_4	370	56	1.0 M KOH	10
IrO_2	481	238	1.0 M $HClO_4$	11
Pt	420	~	1.0 M KOH	12

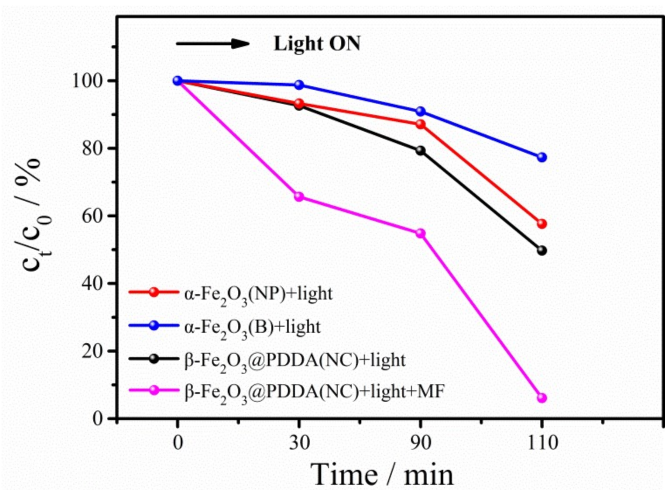

Figure S10. Line chart of RhB concentration (C/C_0) changing with irradiation time.

Table S3. Comparison of several iron oxide based photocatalysis for RhB degradation reported in recent years.

Photocatalysts	Degradation time (min)	Degradation percentage of the RhB dye (%)	Reference.
β-Fe_2O_3@PDDA NC (magnetic-field-enhanced)	110	94	This work
β-Fe_2O_3@PDDA NC	110	50	This work
α-Fe_2O_3 NP	110	42	This work
α-Fe_2O_3 B	110	23	This work
pure α-Fe_2O_3	120	56	[13]
PANI/α-Fe_2O_3/FeOOH	120	91	[13]
α-Fe_2O_3	100	60	[14]
α-Fe_2O_3/RT(0 mM)	100	76	[14]
α-Fe_2O_3/RT(0.025 mM)	100	93	[14]

References

1. O. Alduhaish, M. Ubaidullah, A. M. Al-Enizi, N. Alhokbany, S. M. Alshehri and J. Ahmed, *Sci Rep*, 2019, **9**, 14139.
2. S. Arumugam, Y. Toku and Y. Ju, *Sci Rep*, 2020, **10**, 5407.
3. U. Farooq, P. Chaudhary, P. P. Ingole, A. Kalam and T. Ahmad, *ACS Omega*, 2020, **5**, 20491-20505.
4. A. Samanta, S. Das and S. Jana, *ACS Sustain. Chem. Eng.*, 2019, **7**, 12117-12124.
5. D. Friebel, M. W. Louie, M. Bajdich, K. E. Sanwald, Y. Cai, A. M. Wise, M. J. Cheng, D. Sokaras, T. C. Weng, R. Alonso-Mori, R. C. Davis, J. R. Bargar, J. K. Norskov, A. Nilsson and A. T. Bell, *J Am Chem Soc*, 2015, **137**, 1305-1313.

6. T. Han, Y. Chen, G. Tian, J. Q. Wang, Z. Ren, W. Zhou and H. Fu, *Nanoscale*, 2015, **7**, 15924-15934.
7. Y. Zhao, X. Jia, G. Chen, L. Shang, G. I. Waterhouse, L. Z. Wu, C. H. Tung, D. O'Hare and T. Zhang, *J Am Chem Soc*, 2016, **138**, 6517-6524.
8. H.-Y. Wang, Y.-Y. Hsu, R. Chen, T.-S. Chan, H. M. Chen and B. Liu, *Adv. Energy Mater.*, 2015, **5**, 1500091.
9. H. Tüysüz, Y. J. Hwang, S. B. Khan, A. M. Asiri and P. Yang, *Nano Res.*, 2012, **6**, 47-54.
10. C.-C. Lin and C. C. L. McCrory, *ACS Catal.*, 2016, **7**, 443-451.
11. L. Ouattara, S. Fierro, O. Frey, M. Koudelka and C. Comninellis, *J Appl Electrochem*, 2009, **39**, 1361-1367.
12. C. K. Ranaweera, C. Zhang, S. Bhoyate, P. K. Kahol, M. Ghimire, S. R. Mishra, F. Perez, B. K. Gupta and R. K. Gupta, *Mater. Chem. Front.*, 2017, **1**, 1580-1584.
13. R. Qin, L. Hao and J. Li, *J. Inorg. Organoment. Polym. Mater*, 2020, **30**, 4452-4458.
14. Z. Zhou, H. Yin, Y. Zhao, J. Zhang, Y. Li, J. Yuan, J. Tang and F. Wang, *Catalysts*, 2021, **11**, 396.